Combustion and Flame 221 (2020) 64–73

Contents lists available at ScienceDirect

Combustion and Flame

journal homepage: www.elsevier.com/locate/combustflame

The auto-ignition boundary of ethylene/nitrous oxide as a promising monopropellant

Meng Yang[a], Yue Yang[a], Caiyue Liao[a], Chenglong Tang[a,*], Chong-Wen Zhou[b], Zuohua Huang[a]

[a] State Key Laboratory of Multiphase Flow in Power Engineering, Xi'an Jiaotong University, Xi'an 710049, China
[b] School of Energy and Power Engineering, Beihang University, Beijing 100191, China

ARTICLE INFO

Article history:
Received 13 June 2020
Revised 18 July 2020
Accepted 20 July 2020

Keywords:
C_2H_4/N_2O
Rapid compression machine
Auto-ignition boundary
Ignition delay times

ABSTRACT

C_2H_4/N_2O has recently been proposed as a promising monopropellant for hydrazine replacement. In this work, the auto-ignition capability of argon diluted C_2H_4/N_2O was experimentally investigated firstly in a rapid compression machine by detecting the light emission and the pressure evolution profiles. The auto-ignition boundary temperature which separates the non-ignition and successful ignition cases was then determined and modeled as a function of pressure and mixture composition. Results show that the auto-ignition temperature decreases with the increase of pressure and increases with the argon dilution fraction and fuel oxidizer ratio. In addition, for successful auto-ignition cases, the ignition delay times were measured and used to validate several recently developed kinetic mechanisms. A mechanism was developed and showed good agreement with the measured ignition delay time as well as the auto-ignition boundary temperature at all test conditions. Finally, the auto-ignition boundary temperatures at practical rocket engine conditions (without dilution) were numerically predicted at various pressure and fuel oxidizer ratio conditions. The model is of merit for designing the cooling system and the local flow residence time to reduce the risk of fuel line explosion and the resonance acoustic induced combustion instability in practical rocket engine.

© 2020 The Combustion Institute. Published by Elsevier Inc. All rights reserved.

1. Introduction

Over the years hydrazine and its derivatives have been used as mono- or part of the bi-propellants for space applications, such as in launching vehicles, for satellite attitude control, and as orbit maneuvers. However, due to its extreme toxicity, corrosiveness and high cost in fueling and handling, proposals for the so-called "green propellant" for hydrazine replacement have been emerging, as reviewed by Sackheim and Masse [1] and Gohardani and co-workers [2]. Representative green propellant candidates include hydrogen peroxide [3,4], AND (ammonium dinitramide) or HAN (hydroxylammonium nitrate) based propellants [5], and ionic liquids [6,7]. Each candidate of green propellants may be suitable for a specific propulsion scenario.

Recently, nitrous oxide and fuel blends (NOFB or NOFBX) has raised significant research interests [8–11] due to their superior advantages as monopropellant. Ethylene and nitrous oxide (C_2H_4/N_2O), a typical NOFB combination, has similar vapor pressures, and assures good miscibility and simultaneous evaporation and premixing in one tank. The high vapor pressure (31.2 bar @273 K) also offers self-pressurizing without external pressure supply [12]. More importantly, C_2H_4/N_2O has higher specific impulse (~303 s), potentially low cost, low toxicity and not carcinogenic [1,2,13,14]. As such, investigations on the combustion, flashback and detonation behaviors of C_2H_4/N_2O have been recently conducted.

Werling et al. from the German Aerospace Center's (DLR) conducted the combustion tests with premixed C_2H_4/N_2O and they showed that characteristic exhaust velocity and combustion efficiency of the propellant depends on the oxidizer fuel ratio and chamber length [13]. They also proposed that the flashback risk of this monopropellant needs to be considered and they then designed the injection system equipped with porous elements to avoid flashback [8,9]. Premixed C_2H_4/N_2O has also recently been proposed for their potential applications in pulsed breakdown and detonation driven thrusters. Hageman et al. [10] investigated the detonation behaviors for C_2H_4/N_2O and the measured detonation velocities agree well with the theoretical Chapman-Jouget predictions. Venkatesh et al. [15] experimentally investigated the detonation characteristics of C_2H_4/N_2O and C_2H_2/N_2O. Their

* Corresponding author.
E-mail address: chenglongtang@mail.xjtu.edu.cn (C. Tang).

https://doi.org/10.1016/j.combustflame.2020.07.024
0010-2180/© 2020 The Combustion Institute. Published by Elsevier Inc. All rights reserved.

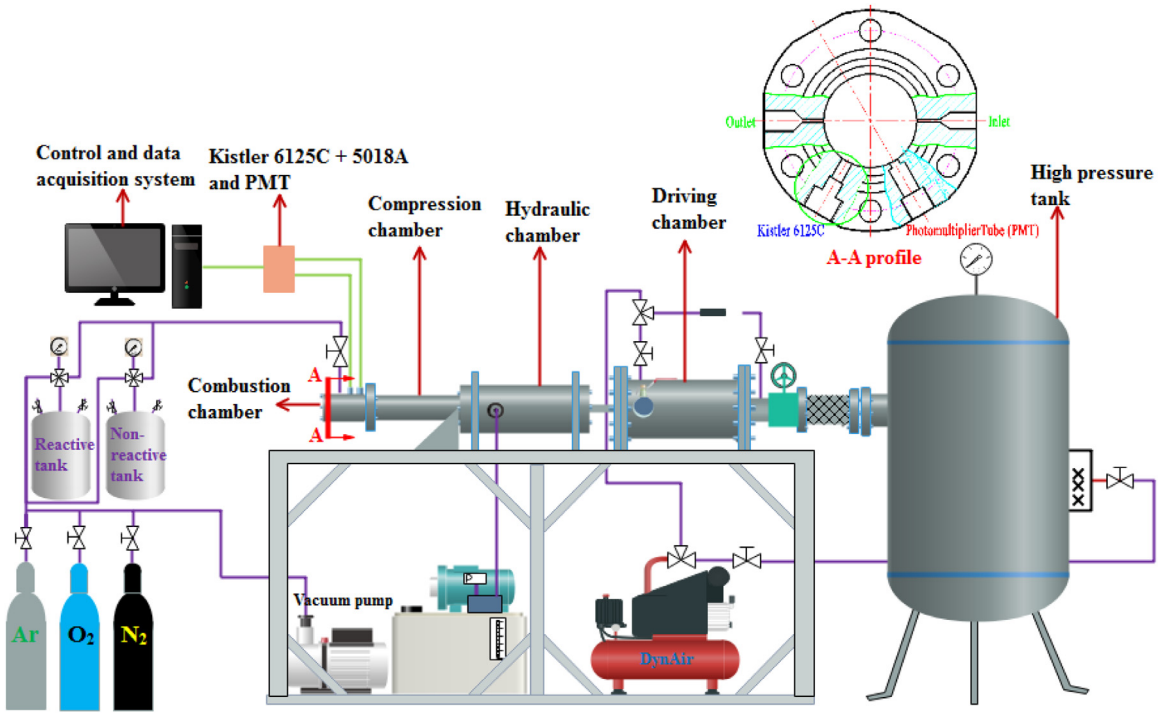

Fig. 1. The schematic of rapid compression machine.

Table 1
Test conditions and reactant mixtures.

Mix	ϕ	C_2H_4/N_2O ratio	C_2H_4 (%)	Ar (%)	p_c (bar)
1	1	1/6	0.25	98.25	15, 20, 25, 30, 35, 40, 45
2	0.5	1/12	0.25	96.75	15, 20, 25, 30, 35, 40, 45
3	2	1/3	0.5	98.00	15, 20, 25, 30, 35, 40, 45
4	1	1/6	0.5	96.50	15, 20, 25, 30, 35, 40, 45
5	2	1/3	1.0	96.00	15, 20, 25, 30, 35, 40, 45

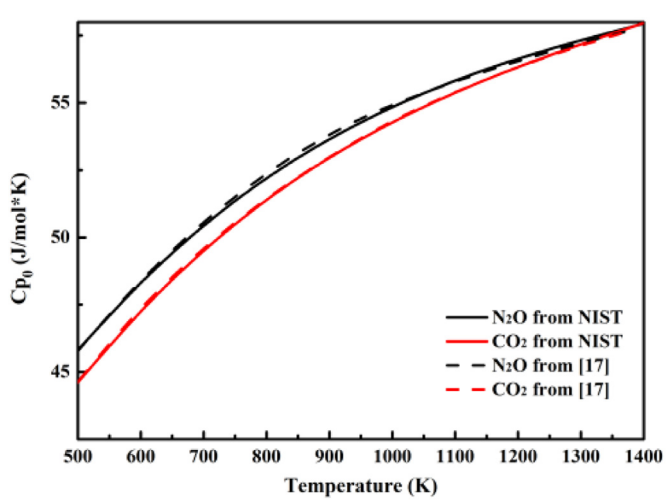

Fig. 2. Comparison of the specific heat between N_2O and CO_2.

measurements showed that C_2H_4/N_2O produces higher average peak pressure than $C_2H_2/$ N_2O, which is contrary to CJ calculations. The higher starting pressure ahead of the combustion wave caused by stronger pre-compression of C_2H_4/N_2O explains this disagreement. Fundamental combustion parameters have also been recently reported. Specifically, Naumann et al. [16] measured ignition delay times $C_2H_4/N_2O/N_2$ mixtures using a shock tube and the laminar flame speeds using a preheat burner of at ambient and elevated pressures. Wang and Zhang [17] measured the laminar flame speeds of C_2H_4/N_2O by using spherically expanding flames at 0.5–2.0 bar and 280 K. Mével and Shepherd [18] measured the ignition delay times of small hydrocarbon (CH_4, C_2H_6, C_2H_4, C_2H_2)-N_2O mixtures with/without the presence of O_2 through a shock tube in the temperature and pressure ranges of 1399–1773 K and 2.54–3.48 bar, respectively. These studies provide important combustion data for validation of kinetic mechanisms.

Attractive as this propellant combination is, the risk associated with the auto-ignition of C_2H_4/N_2O is raised due to the ready reactivity of the fuel/oxidizer mixtures. In the event of accidental leakage, these premixed reactants are readily auto-igniting in the surrounding working environment [1], which induces the risk of explosion or detonation through compression. In addition, in monopropellant rocket engines, local reactive mixtures in the upstream of the burning surface may be heated to its auto-ignition condition if residence time is comparable to the ignition delay time. This local auto-ignition may reinforce the combustion-to-acoustic-field energy transfer processes, which is one source to excite the resonance acoustic mode combustion instability [19]. Thus, auto-ignition needs to be minimized and the auto-ignition boundary should be scrutinized. On the other hand, in certain circumstances auto-ignition needs to be promoted. For instance, the auto-ignition capability and the critical thermodynamic conditions have been modeled to predict the performance of micro-propulsion systems [20]. And the auto-ignition model is also important for designing the staged-bipropellant rocket com-

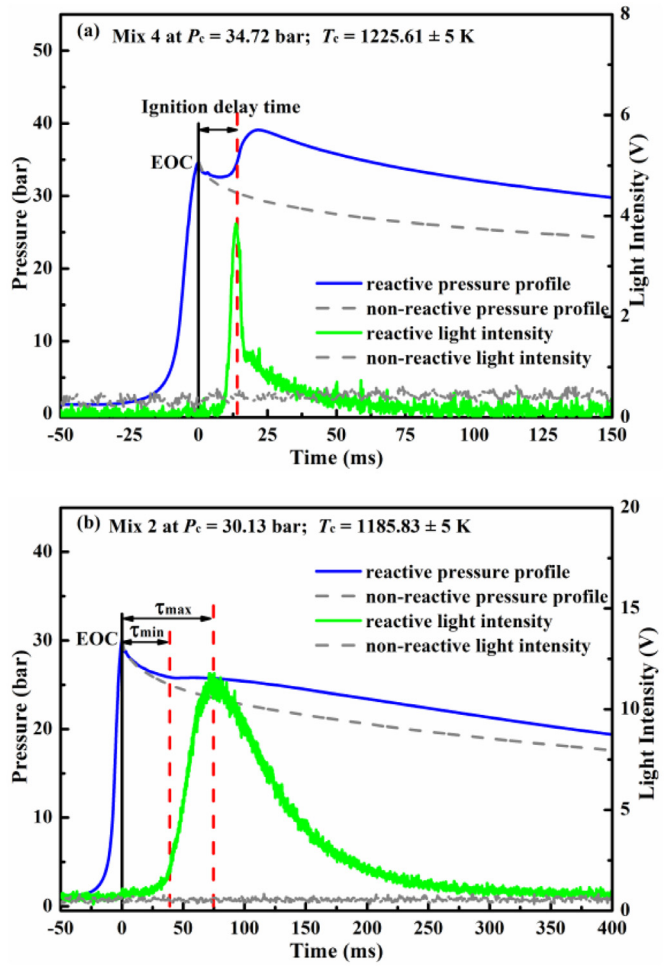

Fig. 3. Typical pressure and light intensity evolution profiles and definitions of ignition delay time.

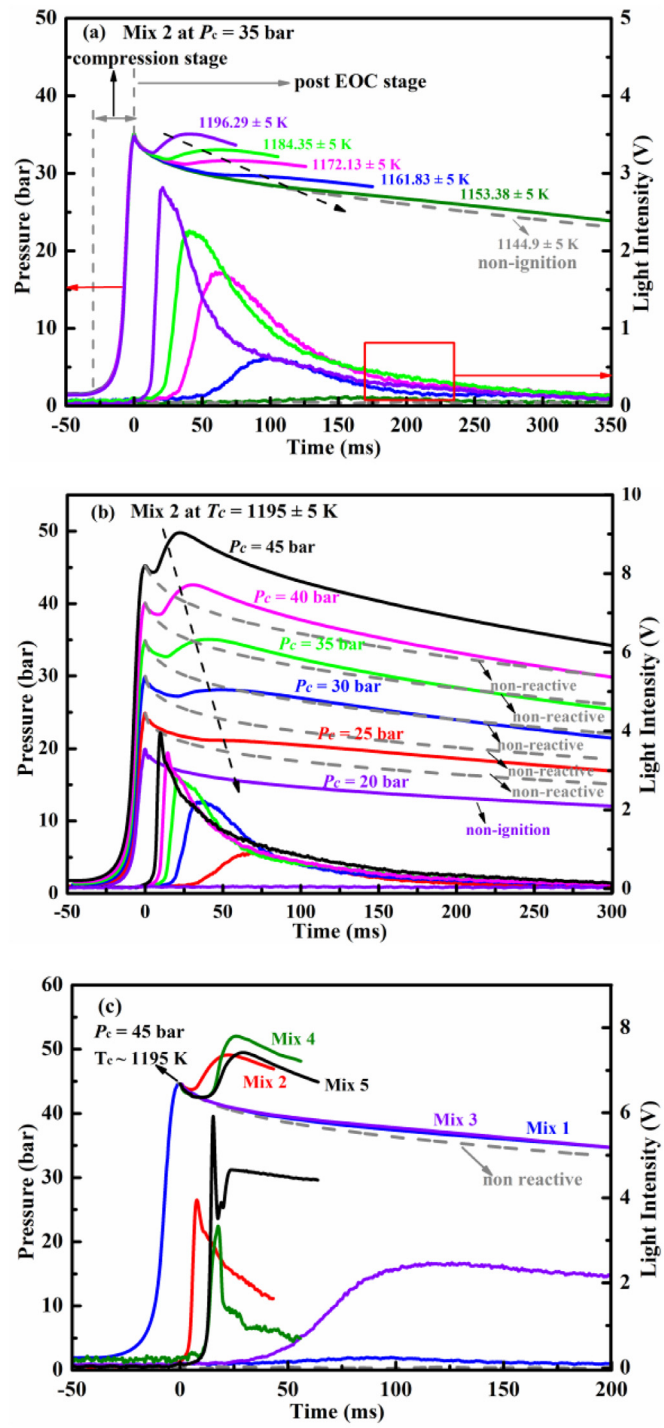

Fig. 4. Raw pressure and light intensity profiles at: (a) different EOC temperatures; (b) different EOC pressures; (c) different mixtures.

bustor, in which successful auto-ignition needs to be promoted [21].

However, as reviewed by Gohardani and co-workers [2], little is known about the auto-ignition properties of NOFB, and limited data has been reported regarding the sensitivity of NOFB, especially under compression. As such, it is of merit to determine the auto-ignition boundary of a premixed NOFB. We note that this boundary describes the lowest pressure or temperature that a given composition of C_2H_4/N_2O will auto-ignite after certain period of induction time (ignition delay time). In addition, it is expected that the auto-ignition capability depends on a variety of thermo physical parameters, including the initial pressure, temperature, and reactant species that govern the auto-ignition chemical kinetics, and the heat loss that may affect the local thermal activation of reactive species. Our objective of this work is to determine the auto-ignition boundary of various C_2H_4/N_2O mixtures. We first experimentally determine the auto-ignition boundaries for the argon diluted C_2H_4/N_2O mixture by using photomultiplier (PMT) detection and a dynamic pressure transducer in a rapid compression machine. In addition, since there have been no data for the ignition delay time of C_2H_4/N_2O mixtures measured by a rapid compression machine facility, we then provide ignition delay time data of $C_2H_4/N_2O/Ar$ mixture over a wide range of conditions. These data, together with the measured auto-ignition boundaries are used for kinetic mechanism validation. Finally, by using a refined and the validated kinetic mechanism, the auto-ignition boundaries at engine relevant fuel oxidizer ratio conditions (without inert dilution) are numerically calculated.

2. Experimental specifications

Experiments were conducted using a recently updated and well validated rapid compression machine (RCM). Fig. 1 shows the schematic diagram of the RCM system. Details of the system can be found in Refs. [22,23]. Briefly, the RCM is a single piston, pneumatically driven and hydraulically stopped machine, which compresses a premixed reactant species to the designed pressure and temper-

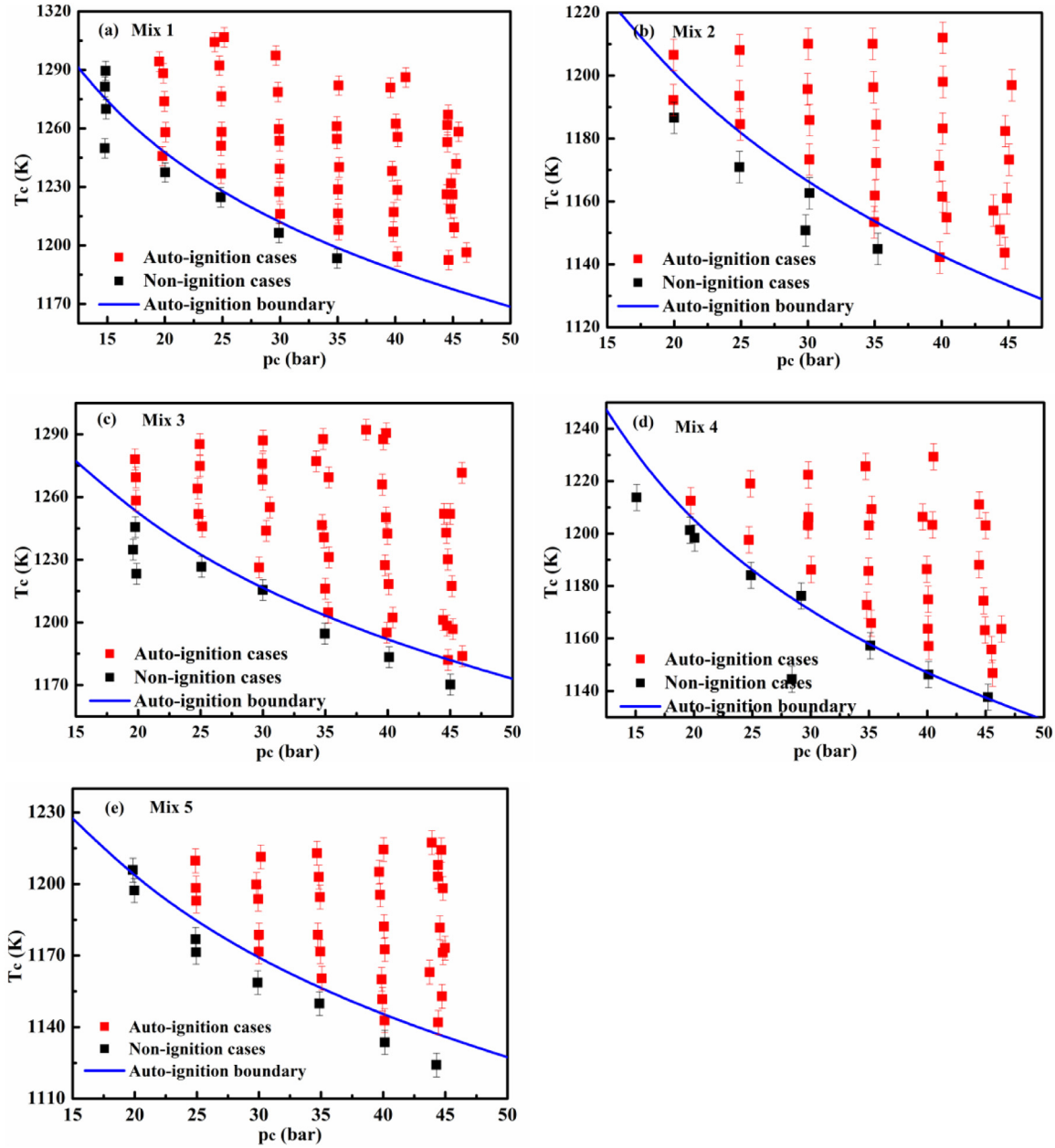

Fig. 5. Test points about ignition at different conditions and the fitting of auto-ignition boundary.

ature for auto-ignition investigation. A combustion chamber with optical access was adopted. The pressure evolution in the chamber is recorded by a piezoelectric pressure transducer (Kistler 6125C) and a charge amplifier (Kistler 5018A). A quartz window (Transmittance 98%) of $\phi = 10$ mm is mounted on the side wall of the combustion chamber. The quartz window port is connected with the PMT (PMTH-S1-CR131) using an optical fiber. As such, the light signal of auto-ignition is detected. In addition, a transconductance amplifier (ZAMP-A) is connected to the PMT output port and the collected optical signal is recorded together with the pressure signal in a data acquisition system. A creviced piston is employed to avoid roll-up vortices and ensure the validity of adiabatic core assumption [23]. By changing the length of the combustion chamber, different compression ratios can be realized.

The reactive and non-reactive mixtures are prepared in two heated stainless vessels according to the partial pressure of each component. The initial temperature is set as 350.15 K. It is noted that for reactive mixture $C_2H_4/N_2O/Ar$, the N_2O is used as an oxidant. The thermodynamic data of the species, obtained from the therm.dat in Ref. [17], shows good agreement with National Institute of Standard and Technology (NIST) data. Since N_2O has almost the same specific heat as CO_2, as shown in Fig. 2, the corresponding non-reactive mixture experiments were conducted by replacing N_2O by CO_2 to obtain the non-reactive volume-time profiles. High purity C_2H_4 (99%), N_2O (99.95%), Ar (99.99%) and CO_2 (99.99%) were used in experiments. The compositions of test gas mixtures are tabulated in Table 1.

The desired compressed conditions in this work can be achieved by changing initial pressure and the compression ratio. The end of compression (EOC) temperature (T_c) is deduced using the initial temperature (T_0), pressure (p_0), the EOC pressure (p_c) and the specific heat ratio (γ) from adiabatic core hypothesis [24]:

$$\int_{T_0}^{T_c} \frac{\gamma}{\gamma - 1} \frac{dT}{T} = \ln\left(\frac{P_c}{P_0}\right)$$

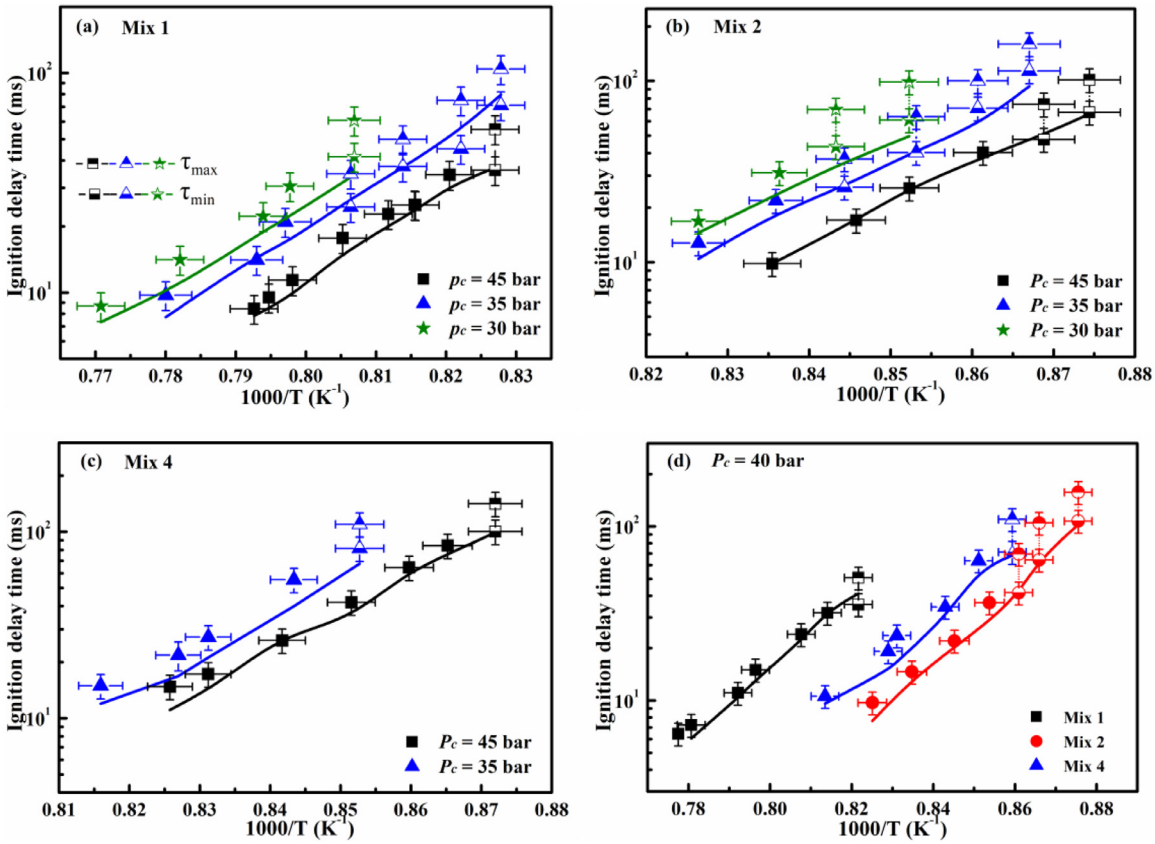

Fig. 6. Experimental and simulated ignition delay times of C_2H_4/N_2O: Symbols: measured ignition delay times; solid lines: predictions using the present mechanism.

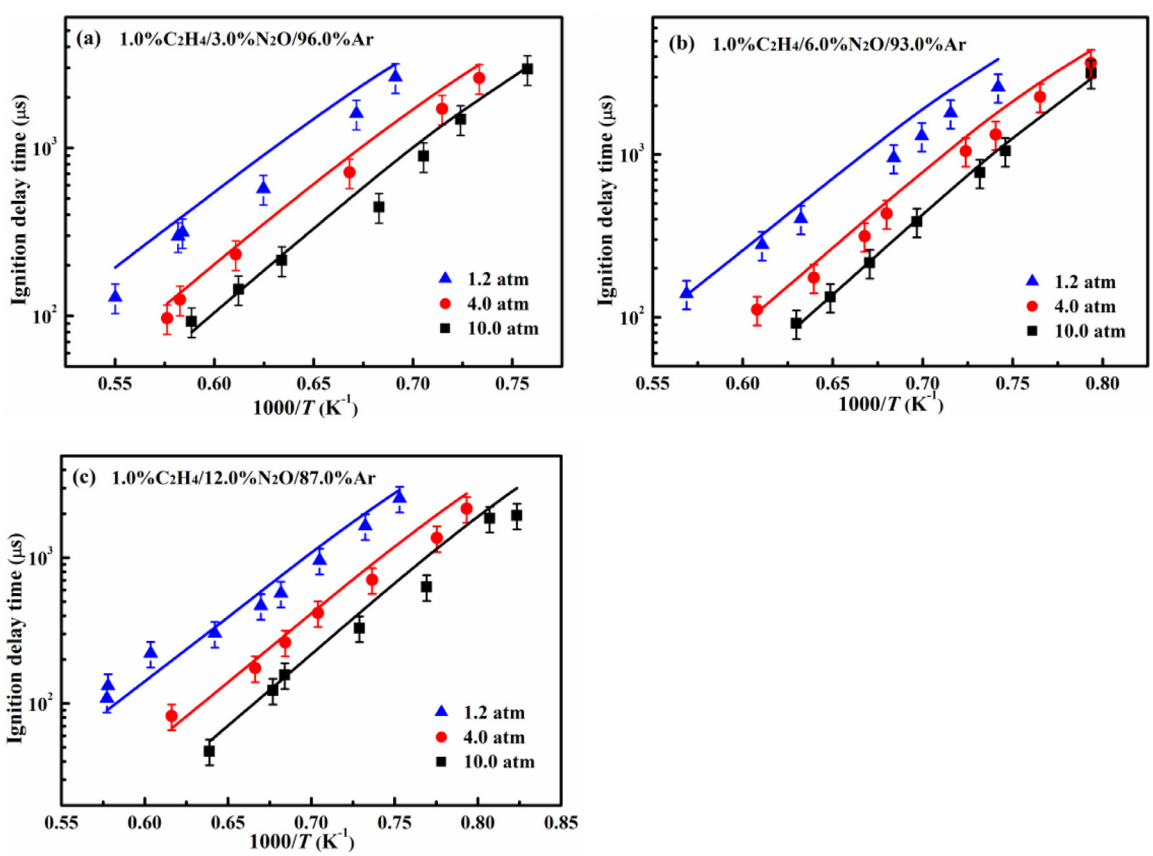

Fig. 7. Comparison between the predicted results and experimental data [30] of high temperature ignition delay times at different equivalence ratios and pressures: Symbols: measured ignition delay times; solid lines: predictions using the present mechanism.

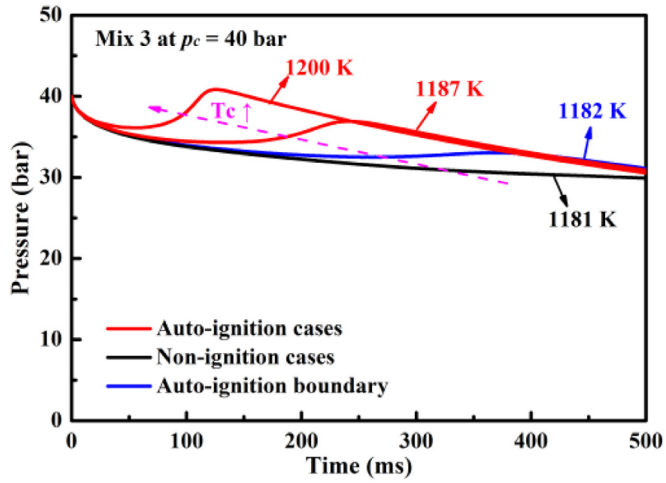

Fig. 8. The identity of simulated auto-ignition boundary for Mix 3 at p_c = 40 bar for the present mechanism.

According to our previous works [22,25], and the Tsinghua RCM results [26], the uncertainty in the estimated EOC temperature is about ±5 K.

By recording the light intensity and the pressure evolution of the combustion chamber, the ignition delay times of $C_2H_4/N_2O/Ar$ can be readily identified. We note that a 430 nm narrow band pass filter together with the photomultiplier was tested, through which we hope to capture the CH* emission. However, the CH* signal was too weak to identify auto-ignition. By tuning the EOC pressures and temperatures, auto-ignition boundaries can be determined. For successful auto-ignition case, there may be strong pressure rise or weak pressure rise, as shown by the two typical cases in Fig. 3a and b. However, there will always be a peak on the light intensity evolution profile. For the strong auto-ignition case, the ignition delay time defined by the maximum pressure rise rate is consistent with the peak light intensity. For the weak auto-ignition case, the pressure rise is slow and a well-defined ignition onset from the pressure profile is not possible. Ignition onset is then in between the onset of the light intensity rise and the peak. As such the minimized and maximized ignition is determined as τ_{min} and τ_{max}. In addition, ignition delay time measurements uncertainties for the RCM have been estimated to be around 15% [22,25].

3. Results and discussion

3.1. Measurements of the auto-ignition boundaries for dilution cases

Fig. 4 shows the raw pressure and light intensity profiles of both the reactive and non-reactive cases from the beginning of compression to the end of compression and the post EOC stage. It is seen that for all cases, the compression processes last for around 20 ms with perfect repeatability. For non-reactive cases (CO_2/C_2H_4), the pressure gradually levels off after EOC due to heat loss, and no light signal is detected. For reactive cases (C_2H_4/N_2O), the emitted light signal is detected and the recorded pressures are higher than the non-reactive cases, as shown by the 35 bar, and EOC temperature > 1153 K cases in Fig. 4a. Successful auto-ignitions are identified in these cases. However, for EOC temperatures < 1153 K, neither light emissions nor pressure rises are detected, indicating that the mixtures do not auto-ignite. As such, the auto-ignition boundary is then determined (35 bar, 1153 K for Mix 2). More specifically, Fig. 4a shows that for given pressure and mixture, decreasing the temperature gradually delays the light emission and pressure evolution, indicating that auto-ignition tendency is progressively weakened. When the temperature is below 1153 K, there is no auto-ignition at all. Fig. 4b shows that for given temperature and mixture, decreasing the pressure also delays the light emission and the pressure evolution with a more gentle light intensity and pressure rise. For pressures lower than 20 bar, no more light intensity and pressure rises are detected. This indicates that decreasing pressure inhibits the auto-ignition. Fig. 4c shows that for given pressure and temperature, whether the system successfully auto-ignite depends also on the mixture composition, since for Mix 2, 4, and 5 obvious light emission and pressure rise are detected. For Mix 3, fairly strong light emission is detected though this case has extremely weak pressure rise. For Mix 1, both light intensity and the pressure rise are negligible, indicating that this mixture is near the auto-ignition boundary.

By scanning the pressure, temperature, and the mixture composition, the auto-ignition capability of each condition is determined from the light emission and the pressure evolution histories. By organizing all the auto-ignition capabilities of the tests in the parameter space of the temperature and the pressure, the auto-ignition boundaries for given mixture are then determined, as shown in Fig. 5. It is seen that for all mixtures, on the auto-ignition boundary, the temperature decreases with the increase of pressure. Comparing Fig. 5a and c, the mixture composition effect on the auto-ignition boundary is very limited. Each data point represents a successful and reliable rapid compression at the designed pressure, temperature for given mixture composition. The auto-ignition boundary pressure and the temperature are obtained by interpolating. The experimentally determined auto-ignition temperatures are then fitted as a function of pressure, the fuel oxidizer ratio and the argon dilution ratio, as Eq. (1). It indicates that the minimum temperature (T_c) to trigger auto-ignition increases with the fuel oxidizer ratio and the argon dilution ratio and decreases with the increase of pressure.

$$T_c = 1630.14 \times \left(\frac{X_{C_2H_4}}{X_{N_2O}}\right)^{0.013} \times X_{Ar}^{1.92} \times p_c^{-0.071} \quad (1)$$

$X_{C_2H_4}$—the mole fraction of C_2H_4;
X_{N_2O}—the mole fraction of N_2O;
X_{Ar}—the mole fraction of Ar;

3.2. Kinetic mechanism validation for dilution cases

3.2.1. Ignition delay times

For successful auto-ignition cases, the measured ignition delay times were presented, as shown by the typical cases in Fig. 6. The ignition delay time of $C_2H_4/N_2O/Ar$ is very sensitive for the variety of temperature and increases rapidly with the temperature decreasing. In addition, it can be seen that the ignition delay time for the given mixture decreases with increasing pressure (Fig. 6a–c). The ignition delay times for different mixtures have obvious difference under the same EOC pressure (Fig. 6d).

Chemical kinetic mechanism of C_2H_4/N_2O reactions was developed to validate the experimental data obtained in this work. AramcoMech 3.0 (C0–C4 reactions, including 1104 reactions, 160 species) [27], which has been well-validated by using a wide range of experimental data was firstly selected as ethylene sub-mechanism. The sub-mechanism (765 reactions, 89 species) of NO_x reactions from Glarborg et al. [28] was adopted to describe the combustion behavior of N_2O oxidation. These two sub-mechanisms were combined in this work to simulate the combustion chemistry of C_2H_4/N_2O mixtures. In addition, model simulations in this work were performed using CHEMKIN PRO [29], the maximum dP/dt is employed for the definition of ignition delay times. Volume-time profiles of non-reactive mixtures were introduced into the simulation to account for heat loss during the compression. The predictions of the simulated ignition delay times using the present mech-

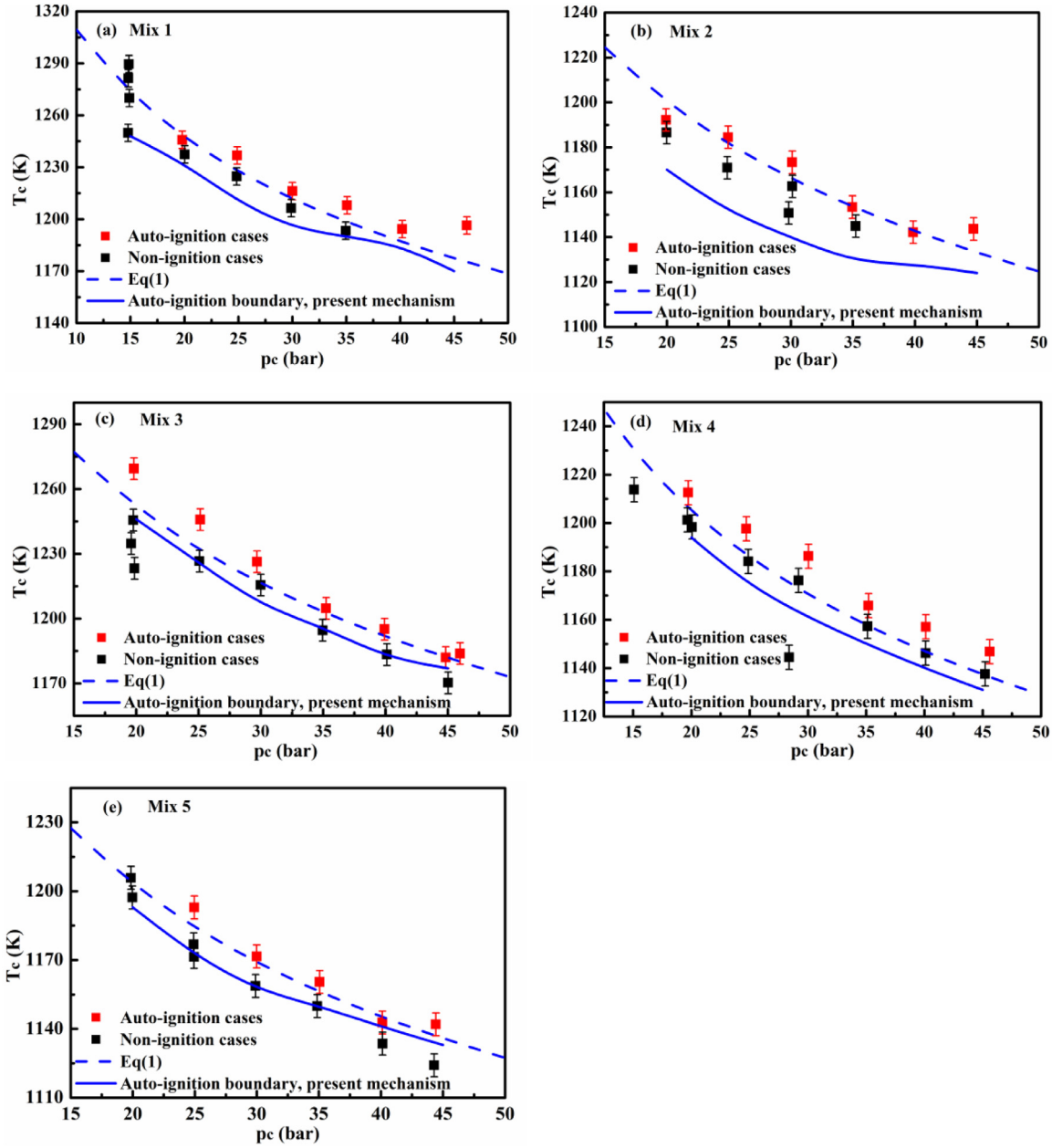

Fig. 9. Comparisons of the experimental, fitted and simulated auto-ignition boundary.

anism (solid lines in Fig. 6) and the measurements are in good agreement.

To further compare and validate the present mechanism of C_2H_4/N_2O established in this work, the high temperature ignition delay times of $C_2H_4/N_2O/Ar$ mixtures in a shock tube [30] were stimulated. As shown in Fig. 7a–c, the present mechanism can predict the high temperature ignition delay times quite well for the mixtures of 1.0% C_2H_4 /3.0% N_2O/96.0% Ar, 1.0% C_2H_4/6.0% N_2O/93.0% Ar and 1.0% C_2H_4 /12.0% N_2O/87.0% Ar over the pressure range investigated.

3.2.2. Auto-ignition boundaries

In the RCM community, for the effect of pressure, main focus is whether the mechanism can predict ignition delay time at different pressures (usually two different pressures) well or not; For the temperature, the main concern is the temperature in the ignition delay times determined from pressure histories range of 10–200 ms. It can be seen that the temperature and pressure of ignition delay time are not related to the auto-ignition limit. So, in this work, we want to introduce another model validation method based on the RCM, which is the validation of auto-ignition boundary. Based on the measurements of the auto-ignition boundaries in Section 3.1, we note that an approximate auto-ignition boundary for $C_2H_4/N_2O/Ar$ mixture at different pressures (15–45 bar) and temperatures can be obtained through light intensity signal. It is difficult to obtain the auto-ignition boundary through the typically pressure measurement in RCM. The auto-ignition boundary reflects the limitation of combustion, which should be captured by the chemical kinetic models. Therefore, the auto-ignition boundaries of $C_2H_4/N_2O/Ar$ mixtures are used to further validate the present model. In addition, model simulations of auto-ignition boundary are also adopted 0-D closed homogeneous batch reactors in CHEMKIN PRO [29]. Volume-time profiles of non-reactive mixtures were introduced into the simulation to account for heat loss

during the compression. It is noted Maas and Warnatz [31] indicate that the catalytic effect of the solid wall may affect the determination of ignition limit at high temperature and low pressure. Considering the combustion chamber wall and piston head has low initial temperature (around 350 K) and the short reaction time scale (< 500 ms) in the present RCM, the wall temperature may not rise to sufficiently high to activate the surface reactions. Thus we think there might not be such uncertainty caused by surface reactions. In addition, we tune down the simulated temperature with a step of 1 K, the pressure rise after EOC becomes slower. When the pressure after EOC does not rise ($dP < 0$) anymore at a specific temperature. This temperature is then regarded as the simulated auto-ignition boundary. For instance, Fig. 8 shows the simulated typical pressure evolution profiles using the present mechanism at different temperatures. No pressure rise ($dP < 0$) is observed for temperature of 1181 K, indicating the non-ignition condition. When temperature increases up to 1182 K, a noticeable pressure rise ($dP > 0$) can be observed and the same trend happens for $T > 1182$ K, which indicates the successful auto-ignition for those conditions. Then, the temperature of 1181 K is regarded as the simulated auto-ignition boundary. The experimental measurements of Mix 3 at 40 bar also did not observe the auto-ignition behavior at 1183.31 K which also confirms that the present mechanism can capture the auto-ignition boundary at this condition.

Simulation using the present mechanism against the predicted auto-ignition boundaries of all mixtures has been carried out and shown in Fig 9. It is seen that for Mix 2 the current prediction under estimate the auto-ignition temperature measurements and the empirical fitting using Eq. (1) at different pressures. Meanwhile, the model can predict the auto-ignition boundary temperatures for the other mixtures. In addition, the present model can't predict the auto-ignition behaviors well at low pressure (15 bar). This may due to the effects from the pressure-dependent rate constants and heat loss which has a more significant influence at low pressures. In general, the present model has a relatively good predicted performance for auto-ignition limit, but can be further improved in the future in predicting auto-ignition behaviors of C_2H_4.

Through the above predicted results and analysis, it can be noted that the measured auto-ignition boundary can be used to validate the kinetic mechanism, besides the ignition delay times.

Sensitivity analyses has also been carried out to identify the reactivity controlling reactions in prediction the auto-ignition process. The sensitivity coefficient indicates the effect of the perturbation of the rate constant on the ignition delay times. The sensitivity coefficient of the ith reaction SC_i is calculated through Eq. (2):

$$SC_i = \left(\tau_{2k_i} - \tau_{0.5k_i}\right)/\tau_{k_i} \tag{2}$$

where k_i is the rate constant of the ith reaction, τ_{ki} is the correspondingly computed ignition delay times. A negative SC_i indicates that increasing the rate constant k_i reduces the ignition delay time τ_{ki}, thus the ith reaction plays a promoting role for ignition, and vice versa. As such, by calculating and comparing the sensitivity coefficients for all the reactions, we can find out the most sensitive reactions for the ignition delay time simulation.

Fig. 10 shows the sensitivity analysis for 0.5% C_2H_4/3.0% N_2O/96.5% Ar mixture at 45 bar and 1200 K. The top 15 sensitive reactions are presented in predicting the ignition delay times of C_2H_4/N_2O. It can be seen that the most sensitive reactions are N_2O (+M) = N_2 + O (+M), N_2O + H=N_2 +OH and CO + N_2O = N_2 + CO_2, which are similar with the high temperature ignition [30]. It is because ethylene is more reactive at high temperature and the C_2H_4/N_2O system is inactive at low to intermediate temperature, hence the mixtures have no typical low to intermediate temperature chemical kinetics.

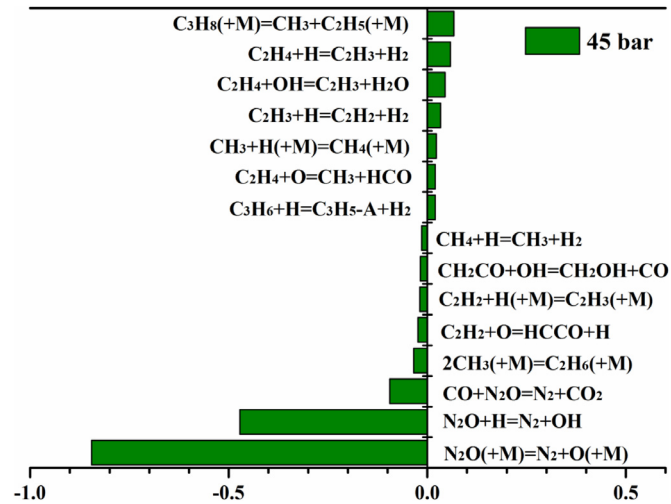

Fig. 10. Normalized sensitivity analysis for the 0.5%C_2H_4/3.0%N_2O/96.5%Ar mixture at 45 bar and 1200 K using the present model.

3.3. Auto-ignition boundary at engine relevant fuel oxidizer ratio conditions

We note that the present RCM can not realize the practical rocket engine-like test conditions because the specific heat ratio of the pure C_2H_4/N_2O blend is large such that the temperature after EOC is too low to lead to the auto-ignition. Heating of the present RCM system has been considered, but the calculated maximum pressure rise and the pressure rise rate upon auto-ignition of pure C_2H_4/N_2O blend is around 200 bar (at $p_c = 45$ bar, $C_2H_4/N_2O = 1/1$), which is beyond the maximum allowable working pressure of the RCM.

As such, we use the present assemble kinetic mechanism, which has been validated against the ignition delay time and the auto-ignition boundary at the diluted cases to simulate the auto-ignition boundary at engine relevant fuel oxidizer ratio (no dilution) conditions. 0-D closed homogeneous batch reactor is adopted. The mixture composition (C_2H_4/N_2O) and pressure are set as 1/9 and 25–45 bar, respectively. Then we simulate the auto-ignition process through adjust the temperature until the mixture ignites. In this work, the auto-ignition boundary temperature is defined by checking the simulated pressure history within 500 ms. In addition, we set the heat loss example of −0.03 bar/ms to demonstrate and compare the effect of heat loss on the auto-ignition.

Fig. 11 plots the auto-ignition boundary temperature as a function of the fuel oxidizer ratio for different pressures. The solid lines and the dash lines respectively represent the results with considering the heat loss (assumed equivalent to $dP/dt = -0.03$ bar/ms in the inset figure) and for adiabatic compression. It is seen that the auto-ignition temperature at adiabatic condition is lower than that at considering heat loss condition at specific C_2H_4/N_2O ratio. In addition, the auto-ignition boundary temperature decreases with increasing pressure at specific fuel oxidizer ratio. For given pressure, the auto-ignition boundary temperature firstly increases with the fuel oxidizer ratio increases then levels off.

We note that for practical rocket engine, the fuel/oxidizer ratio is in the range between 1/12 and 1/3, and the combustion temperature is as high as 3000 K [8,9]. The cooling system is required to ensure that the propellant tank and the fueling assembly temperature is lower than the auto-ignition boundary temperature. In addition, in the upstream of the burning surface in the practical rocket engine chamber, these unburned mixtures may be heated up by the burning surface beyond its auto-ignition boundary temperature. As such, the local residence time or the Damkohler number

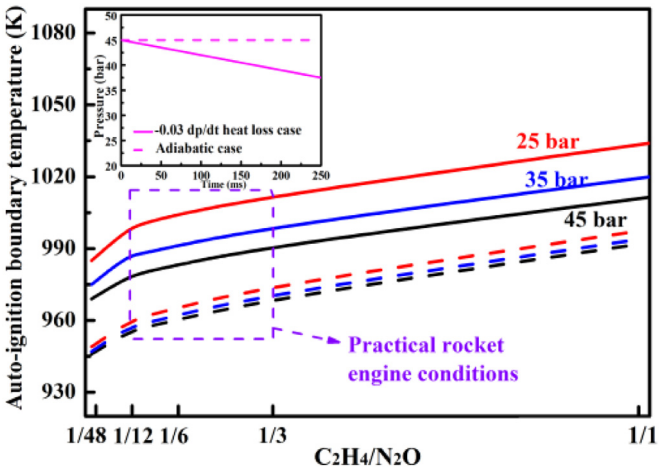

Fig. 11. Simulated auto-ignition boundary temperature for C_2H_4/N_2O blend under no dilution conditions (solid lines: considering heat loss cases; dash lines: adiabatic cases).

needs to be carefully designed to avoid the local auto-ignition. Because this auto-ignition is believed to reinforce the combustion-to-acoustic-field energy transfer processes and excite the resonance acoustic modes combustion instability [19].

4. Conclusions

In this work, we have firstly investigated the auto-ignition capability of argon diluted C_2H_4/N_2O over wide range of pressure, temperature and mixture compositions in a heated rapid compression machine. By examining the pressure and the light emissions at various pressures, temperatures and mixture composition, the auto-ignition boundaries were determined and modeled. Results show that the auto-ignition boundary temperature decreases with the fuel/oxidizer ratio and the argon dilution ratio, but decreases with the increase of pressure. Secondly, the ignition delay times for successful auto-ignition cases were used to validate the established mechanism. The mechanism shows better agreement with both the measured ignition delay time and the auto-ignition boundary. Finally, auto-ignition boundaries with/without heat loss at practical engine relevant fuel oxidizer ratio conditions (without dilution and beyond the experimental facility limit) were numerically predicted by using the present mechanism. The predicted auto-ignition boundary is hoped to provide some guidance for designing the fuel line cooling system to avoid explosion and the local flow residence time organization to minimize the resonance acoustic combustion instability in practical rocket engines.

Declaration of Competing Interest

The authors declare that they have no known competing financial interests or personal relationships that could have appeared to influence the work reported in this paper.

Acknowledgements

This work is supported by the National Natural Science Foundation of China (51722603), and the Fundamental Research Funds for the Central Universities. Chong-Wen Zhou acknowledges the funding support from National Science and Technology Major Project (2017-III0004-0028).

Supplementary materials

Supplementary material associated with this article can be found, in the online version, at doi:10.1016/j.combustflame.2020.07.024.

References

[1] R.L. Sackheim, R.K. Masse, Green propulsion advancement: challenging the maturity of monopropellant hydrazine, J. Propul. Power 30 (2014) 265–276.
[2] A.S. Gohardani, J. Stanojev, A. Demairé, K. Anflo, M. Persson, N. Wingborg, C. Nilsson, Green space propulsion: opportunities and prospects, Prog. Aerosp. Sci. 71 (2014) 128–149.
[3] O. Božić, D. Porrmann, D. Lancelle, S. May, Enhanced development of a catalyst chamber for the decomposition of up to 1.0 kg/s hydrogen peroxide, CEAS Space J. 8 (2016) 77–88.
[4] U. Gotzig, Development and test of a 3D printed hydrogen peroxide flight control thruster, 51st AIAA/SAE/ASEE Joint Propulsion Conference, 2015.
[5] T. Katsumi, J. Nakatsuka, K. Hasegawa, K. Kobayashi, S. Sawai, K. Hori, HAN-based green propellant, application, and its combustion mechanism, Combust. Explos. Shock Waves 48 (2012) 536–543.
[6] S.P. Berg, J.L. Rovey, Assessment of imidazole-based ionic liquids as dual-mode spacecraft propellants, J. Propuls. Power 29 (2013) 339–351.
[7] J.L. Shamshina, S. Marcin, D.M. Drab, P.T. G.annon, H.W.H. Dykes, D.S. Roberto, A.J. Reich, R.D. Rogers, Catalytic ignition of ionic liquids for propellant applications, Chem. Commun. 46 (2010) 8965–8967.
[8] L. Werling, Y. Jooss, M. Wenzel, H. Clezki, S. Schlechtriem, A premixed green propellant consisting of N_2O and C_2H_4: experimental analysis of quenching diameters to design flashback arresters, Int. J. Energy Mater. Chem. Propul. 17 (2018) 241–262.
[9] L. Werling, A. Hauk, S. Miiller, H. Clezki, S. Schlechtriem, Pressure drop measurement of porous materials: flashback arrestors for a N_2O/C_2H_4 premixed green propellant, 52nd AIAA/SAE/ASEE Joint Propulsion Conference, 2016.
[10] M.D. Hageman, D.R. Hopper, M.S. Knadler, Detonation limits and velocity deficits of CH_4, C_2H_4, C_2H_6 and C_3H_8 with N_2O in a small diameter tube, AIAA Propulsion and Energy 2019 Form, 2019.
[11] M. Vozoff, G. Mungas, NOFBTM: a non-toxic, “Green” propulsion technology with high performance and low cost, AIAA SPACE 2012 Conference & Exposition, 2012.
[12] S.A. Whitmore, S.N. Chandler, Engineering model for self-pressurizing saturated-N_2O-propellant feed systems, J. Propul. Power 26 (2010) 706–714.
[13] L.K. Werling, M. Hassler, F. Lauck, H.K. Ciezki, S. Schlechtriem, Experimental performance analysis (c^* & c^* efficiency) of a premixed green propellant consisting of N2O and C2H4, 53rd AIAA/SAE/ASEE Joint Propulsion Conference, 2017.
[14] O.A. Powell, J.E. Miller, C. Dreyer, P. Papas, Characterization of hydrocarbon/nitrous oxide propellant combinations, 46th AIAA Aerospace Sciences Meeting and Exhibit, 2008.
[15] P.B. Venkatesh, S.E. Meyer, S.P.M. Bane, M.C. Grubelich, Deflagration-to-detonation transition in nitrous oxide/oxygen-fuel mixtures for propulsion, J. Propul. Power 35 (2019) 944–952.
[16] C. Naumann, T. Kick, T. Methling, M. Braun-Unkhoff, U. Riedel, Ethene/dinitrogen oxide - A green propellant to substitute hydrazine: investigation on its ignition delay time and laminar flame speed, 26th International Colloquium on the Dynamics of Explosions and Reactive Systems, 2017.
[17] W. Wang, H. Zhang, Laminar burning velocities of C_2H_4/N_2O flames: experimental study and its chemical kinetics mechanism, Combust. Flame 202 (2019) 362–375.
[18] R. Mével, J.E. Shepherd, Ignition delay-time behind reflected shock waves of small hydrocarbons-nitrous oxide(-oxygen) mixtures, Shock Waves 25 (2015) 217–229.
[19] B. Chehroudi, Physical hypothesis for the combustion instability in cryogenic liquid rocket engines, J. Propul. Power 26 (2010) 1153–1160.
[20] M. Schiebl, A. Woschnak, D. Krejci, F. Winte, C. Scharlemann, Modeling of jet A1-H_2O_2 autoignition in a microrocket combustion chamber, J. Propul. Power 29 (2013) 385–395.
[21] J. Sisco, J. Mok, B. Austin, W. Anderson, Autoignition of kerosene by decomposed peroxide in a dump combustor configuration, 39th AIAA/ASME/SAE/ASEE Joint Propulsion Conference and Exhibit, 2003.
[22] M. Yang, Y. Wu, C. Tang, Y. Liu, Z. Huang, Auto-ignition behaviors of nitromethane in diluted oxygen in a rapid compression machine: critical conditions for ignition, ignition delay times measurements, and kinetic modeling interpretation, J. Hazard. Mater. 377 (2019) 52–61.
[23] Y. Wu, M. Yang, C. Tang, Y. Liu, P. Zhang, Z. Huang, Promoting "adiabatic core" approximation in a rapid compression machine by an optimized creviced piston design, Fuel 251 (2019) 328–340.
[24] G. Mittal, C.-J. Sung, A rapid compression machine for chemical kinetics studies at elevated pressures and temperatures, Combus. Sci. Technol. 179 (2007) 497–530.
[25] N. Xu, Y. Wu, C. Tang, P. Zhang, X. He, Z. Wang, Z. Huang, Ignition delay times of low alkylfurans at high pressures using a rapid compression machine, Proc. Combust. Inst. 36 (2017) 323–332.

[26] H. Di, X. He, P. Zhang, Z. Wang, M.S. Wooldridge, C.K. Law, C. Wang, S. Shuai, J. Wang, Effects of buffer gas composition on low temperature ignition of iso-octane and n-heptane, Combust. Flame 161 (10) (2014) 2531–2538.
[27] C.-.W. Zhou, Y. Li, U. Burke, C. Banyon, K.P. Somers, S. Ding, S. Khan, J.W. Hargis, T. Sikes, O. Mathieu, E.L. Petersen, M. AlAbbad, A. Farooq, Y. Pan, Y. Zhang, Z. Huang, J. Lopez, Z. Loparo, S.S. Vasu, H.J. Curran, An experimental and chemical kinetic modeling study of 1,3-butadiene combustion: ignition delay time and laminar flame speed measurements, Combust. Flame 197 (2018) 423–438.
[28] P. Glarborg, J.A. Miller, B. Ruscic, S.J. Klippenstein, Modeling nitrogen chemistry in combustion, Prog. Energy Combust. Sci. 67 (2018) 31–68.
[29] R. Design, Chemkin, 2006 URL: http://www.reactiondesign.com/products/chemkin.
[30] F. Deng, Y. Pan, W. Sun, F. Yang, Y. Zhang, Z. Huang, Comparative study of the effects of nitrous oxide and oxygen on ethylene ignition, Energy Fuel 31 (2017) 14116–14128.
[31] U. Maas, J. Warnatz, Ignition processes in hydrogen oxygen mixtures, Combust. Flame 74 (1988) 53–69.